
This is an electronic reprint of the original article.
This reprint may differ from the original in pagination and typographic detail.

Liu, Mengke; Zhao, Yingnan; Zhao, Huawang; Li, Xianghui; Ma, Yuhan; Yong, Xin; Chen, Hong; Li, Yongdan

The promotion effect of nickel and lanthanum on Cu-ZSM-5 catalyst in NO direct decomposition

Published in:
Catalysis Today

DOI:
[10.1016/j.cattod.2018.05.002](https://doi.org/10.1016/j.cattod.2018.05.002)

Published: 01/05/2019

Document Version
Peer-reviewed accepted author manuscript, also known as Final accepted manuscript or Post-print

Published under the following license:
CC BY-NC-ND

Please cite the original version:
Liu, M., Zhao, Y., Zhao, H., Li, X., Ma, Y., Yong, X., Chen, H., & Li, Y. (2019). The promotion effect of nickel and lanthanum on Cu-ZSM-5 catalyst in NO direct decomposition. *Catalysis Today*, 327, 203-209.
<https://doi.org/10.1016/j.cattod.2018.05.002>

This material is protected by copyright and other intellectual property rights, and duplication or sale of all or part of any of the repository collections is not permitted, except that material may be duplicated by you for your research use or educational purposes in electronic or print form. You must obtain permission for any other use. Electronic or print copies may not be offered, whether for sale or otherwise to anyone who is not an authorised user.

The promotion effect of nickel and lanthanum on Cu-ZSM-5 catalyst in NO direct decomposition

Mengke Liu^a, Yingnan Zhao^b, Huawang Zhao^a, Xianghui Li^a, Yuhan Ma^a, Xin Yong^a, Hong Chen^c, Yongdan Li^{ab*}

^a Collaborative Innovation Center of Chemical Science and Engineering (Tianjin), Tianjin Key Laboratory of Applied Catalysis Science and Technology, State Key Laboratory of Chemical Engineering (Tianjin University), School of Chemical Engineering, Tianjin University, Tianjin 300072, China

^b Department of Chemical and Metallurgical Engineering, School of Chemical Engineering, Aalto University, Kemistintie 1, Espoo, P.O. Box 16100 FI-00076 Aalto Finland

^c School of Environmental Science and Engineering, Tianjin University, Tianjin 300072, China

Abstract

A number of M-Cu-ZSM-5 (M=La, Ni, La-Ni) samples were prepared via an aqueous solution ion-exchange method. The co-doping with Ni and La into a Cu-ZSM-5 catalyst enhanced the NO decomposition activity in a temperature range 350-550 °C. The characterization results indicate that doping with La effectively improved the dispersion of the Cu species forming more Cu²⁺ ions in the sample, while the effect of Ni is likely to facilitate the implantation of Cu²⁺ to form (Cu²⁺-O²⁻-Cu²⁺)²⁺ dimers. The synergistic effect of La and Ni contributes to the increased (Cu²⁺-O²⁻-Cu²⁺)²⁺ content in the co-doped sample, thus enhancing the NO decomposition activity.

Keywords: Cu-ZSM-5, NO decomposition, Emission control, Ni and La doping

* Corresponding author: Tel.: +358 46 9214 550; Fax: +86 22 27405234. E-mail address: Yongdan.li@aalto.fi (Y.D. Li).

1. Introduction

The abatement of nitrogen oxide in the exhaust gases, both of mobile and stationary sources, has received extensive research interest, and many technologies were developed such as selective catalytic reduction (SCR), lean NO_x trap and NO decomposition [1-8]. NO direct decomposition to N₂ and O₂ is an ideal route for NO removal because of the simple reacting network with no additional reductant [9]. Nevertheless, NO is stable in gas phase, requiring over 1000 °C to overcome the 364 kJ/mol barriers for the N-O bonding cleavage in thermal decomposition. As a result, a suitable catalyst is critical to overcome the huge energy barrier, lowering the NO decomposition temperature [10].

Ion-exchanged ZSM-5, especially the copper ion-exchanged ZSM-5 (Cu-ZSM-5), has been reported active for NO decomposition in 300-600 °C, whereas the deNO_x activity should be further improved [11, 12]. Doping with additives in Cu-ZSM-5 was considered as an effective method to enhance its NO elimination performance [13-15]. Pârvulescu *et al.* reported that samarium significantly improved the activity of the Cu-ZSM-5 for NO decomposition [14]. Zhang and Flytzani-Stephanopoulos observed enhancement of NO decomposition activity in wet gas streams in 400-600 °C with doping cerium into the Cu-ZSM-5 catalyst [13]. Grange *et al.* prepared Ce, Sn and Tl doped Cu-ZSM-5 with co-exchange method, and found that the presence of a second component led to a better positioning of Cu, resulting in an improvement of the catalytic property [15].

In this work, both La and Ni are used as the promoters to improve the NO decomposition activity of a Cu-ZSM-5 catalyst. The promotion effect of La, Ni on the Cu-ZSM-5 catalyst in NO decomposition reaction will be discussed.

2. Experimental

2.1. Chemicals

Cupric nitrate ($\text{Cu}(\text{NO}_3)_2 > 99 \text{ wt.}\%$) was purchased from Aladdin. Ammonium nitrate ($\text{NH}_4\text{NO}_3 > 99 \text{ wt.}\%$) was purchased from Yuanli. The H-ZSM-5 ($\text{SiO}_2/\text{Al}_2\text{O}_3=25$) was provided by Nankai Catalyst Corporation. All the aqueous solutions were prepared using ultra-pure water (Yongqingyuan Tianjin).

2.2. Preparation of Catalyst

The H-ZSM-5 sample was ion-exchanged in ammonia sulfate solution (2.3 mol/L) at 80 °C for 2 h to form NH_4 -ZSM-5. After filtration, washing and drying at 90 °C for 19 h, 1 g of NH_4 -ZSM-5 was immersed in 0.1 L of $\text{Cu}(\text{NO}_3)_2$ solution (0.01 mol/L) for ion-exchange overnight at ambient temperature at pH 5. Subsequently, the samples were filtrated, washed and dried at 90 °C again, followed by calcination in air at 550 °C for 5 h, for obtaining the Cu-ZSM-5 sample.

1 g of NH_4 -ZSM-5 was dispersed in 0.1 L of $\text{Cu}(\text{NO}_3)_2$ solution (0.01 mol/L) and 0.001 mol/L $\text{La}(\text{NO}_3)_3 \cdot 6\text{H}_2\text{O}$ or 0.002 mol/L $\text{Ni}(\text{NO}_3)_2 \cdot 6\text{H}_2\text{O}$ at room temperature for 24 h, for obtaining the La-Cu-ZSM-5 or Ni-Cu-ZSM-5 samples, respectively. 1 g of NH_4 -ZSM-5 was dispersed in 0.001 mol/L $\text{La}(\text{NO}_3)_3 \cdot 6\text{H}_2\text{O}$ or 0.002 mol/L $\text{Ni}(\text{NO}_3)_2 \cdot 6\text{H}_2\text{O}$ at room temperature for 24 h, for obtaining the La-ZSM-5 or Ni-ZSM-5 samples, respectively. The La-Ni-Cu-ZSM-5 catalyst was prepared with ion-exchange in an aqueous solution containing 0.001 mol/L $\text{La}(\text{NO}_3)_3 \cdot 6\text{H}_2\text{O}$, 0.002 mol/L

Ni(NO₃)₂·6H₂O and 0.01 mol/L Cu(NO₃)₂·3H₂O at room temperature for 24 h. After the ion-exchange, the samples were filtrated, washed, dried, and subsequently calcined in air at 550 °C for 5 h. Finally, all the samples were pelletized, then crushed and sieved afterwards to 40-60 mesh.

2.3. Characterization

The chemical composition of the catalysts was determined with an inductively coupled plasma optical emission spectrometry (ICP-OES, VISTA-MPX, Varian).

The crystalline structure of the commercial zeolite was checked with a D/max-γ b-type X-ray diffractometer (Rigaku) using monochromatic Cu Kα radiation (at 40 kV and 100 mA), with a scan rate of 2 °/min.

The X-ray photoelectron spectroscopy (XPS) was performed on a PHI-1600 ESCA SYSTEM spectrometer using Mg Kα as X-ray source (1253.6 eV) under a residual pressure of 5×10^{-6} Pa. The error of the binding energy is ±0.2 eV using C 1 s at 284.8 eV as the standard.

N₂ physical adsorption at -196 °C was used to determine the surface area and the pore distribution of the catalysts on Quantachrome Autosorb-1, and the micropore volumes was determined using the t-plot method. All the samples were degassed at 300 °C for 6 h prior to the measurement.

The temperature-programmed desorption (TPD) was carried out in a home-built fixed-bed micro-reactor (10 mm in diameter) equipped with a thermal conductivity detector (TCD). For NO-TPD, 0.2 g of sample was loaded in the reactor and pretreated

in He (50 ml/min) at 550 °C for 1 h and then cooled to 50 °C. Subsequently, the sample was exposed to 500 ppm NO/He (500 ml/min) at 50 °C for 1 h. The physical adsorption NO was removed by flushing with He until no NO was detected. Then, the catalyst was heated in He from 50 °C to 550 °C at a rate of 10 °C/min for the NO_x (NO, NO₂, N₂O) desorption.

For the O₂-TPD, 0.2 g of sample was pretreated in 40% O₂/He (30 ml/min) at 500 °C for 8 h, then cooled to room temperature in the same atmosphere. After that, the sample was purged in He (30 ml/min) for 1 h. The temperature was then increased up to 800 °C with a ramp of 10 °C/min for O₂ desorption.

The reducibility of copper in the catalyst was investigated with temperature-programmed reduction with H₂ (H₂-TPR). The experiment was performed on a Micromeritics AutoChem 2910 equipped with a TCD detector. 0.1 g catalyst was loaded into a quartz U-reactor. The catalyst was pretreated in Ar flow (50 ml/min) at 550 °C for 1 h and then cooled down to the room temperature in the same atmosphere. Subsequently, the catalyst was heated in 5 vol.% H₂/Ar (30 ml/min) from room temperature to 800 °C with a ramp of 10 °C/min to perform H₂-TPR.

2.4. NO decomposition performance

The catalysts samples were tested for the decomposition of NO in a fixed-bed reactor (10 mm in diameter) in a steady flow operation. Typically, 0.5 g sample (40-60 mesh) was loaded in the reactor. The sample was preheated in He (20 ml/min) at 500 °C for 2 h. After that, the reaction gas (2 vol.% NO/He) was fed with a flow rate of 20 ml/min

(space velocity = 1200 h⁻¹). The reaction temperature was increased from 350 °C to 550 °C with steps of 50 °C. The NO decomposition activity at 500 °C in different space velocity was obtained with the reaction gas varied from 20 ml/min to 180 ml/min. The outlet composition was monitored with a GC equipped with TCD detector. The NO conversion was calculated with the following equation:

$$\text{NO conversion} = \frac{2 [\text{N}_2]_{\text{out}}}{[\text{NO}]_{\text{in}}} \times 100\% \quad (1)$$

where $[\text{N}_2]_{\text{out}}$ is outlet concentration of the N₂ (ppm), $[\text{NO}]_{\text{in}}$ is inlet concentration of NO (ppm).

The TOF (turn over frequency: number of NO molecules converted to N₂ and O₂ per metal site per second at 2 vol.% NO) data is calculated with formula:

$$\text{TOF} = \frac{X_{\text{NO}}[\%] \times F_{\text{NO}} [\text{L} \cdot \text{min}^{-1}] \times M_{\text{Cu}} [\text{g} \cdot \text{mol}^{-1}]}{m_{\text{catal}} [\text{g}] \times W_{\text{Cu}} [\%] \times 60 [\text{S} \cdot \text{min}^{-1}] \times 22.4 [\text{L} \cdot \text{mol}^{-1}]} \quad (2)$$

where X_{NO} is the conversion of NO, F_{NO} is the flow rate of NO, M_{Cu} is the molar mass of Cu. m_{catal} is the mass of catalyst, W_{Cu} is the mass fraction of Cu in the samples according to the results of ICP.

3. Results

3.1. Structural and textural properties

ICP results show that all samples have the almost identical Cu content in Table 1. Both La, Ni contents in the co-doped La-Ni-Cu-ZSM-5 sample are less than those in the single doped Ni-Cu-ZSM-5 and La-Cu-ZSM-5 samples. Table 2 shows that the surface areas and pore volumes decreased with the further doped samples as compared to those of the Cu-ZSM-5 sample. Fig. 1 shows the micropore size distribution of NH₄-ZSM-5 sample determined with the Horvath-Kawazoe methods. The pore size is mainly concentrated at 5.0 Å.

As shown in Fig. 2, all the catalyst samples exhibit typical diffraction pattern of the ZSM-5 zeolite structure with a high degree of crystallization (PDF#44-0003) [9, 16]. The diffraction peaks for CuO (PDF#45-0937) are also clearly observed in La-Ni-Cu-ZSM-5, Ni-Cu-ZSM-5, La-Cu-ZSM-5 and Cu-ZSM-5 samples, as shown in the insert of the Fig.2 [9, 16]. However, no other crystalline phases involving Ni or La can be identified with XRD, which illustrates their well dispersion over the ZSM-5 structure or too small size under detection limitation.

3.2 O₂-TPD

Three desorption peaks were observed in the O₂-TPD curve of Cu-ZSM-5 in the temperature range below 550 °C, at around 100, 250, and 350 °C, respectively, as shown in Fig. 3. These peaks at 100 and 250 °C can be assigned to the desorption molecularly adsorbed oxygen species and the O₂ desorption on Cu²⁺ monomers, respectively [17,

18]. The peak at 350 °C was ascribed to the O₂ desorption from (Cu²⁺-O²⁻-Cu²⁺)²⁺ sites, which was referred to the Cu-dimer sites in dynamic transformation with the (Cu⁺-□- Cu⁺)²⁺ (□ = oxygen vacancy) sites [17, 18]. In addition, the peak with the highest temperature at around 720 °C was assigned to the lattice oxygen desorption, indicating collapse of the molecular sieve skeleton at such a high temperature [18]. The desorption peak positions of the La-Cu-ZSM-5 and Ni-Cu-ZSM-5 samples are very similar to those of the Cu-ZSM-5 sample. Nevertheless, the O₂ desorption peaks from the Cu²⁺ monomers and (Cu²⁺-O²⁻-Cu²⁺)²⁺ sites shift to lower temperatures at around 240 and 330 °C, respectively, with the La-Ni-Cu-ZSM-5 sample.

3.3. H₂-TPR

The reduction of Cu²⁺ ions (including the Cu²⁺ monomers and the (Cu²⁺-O²⁻-Cu²⁺)²⁺ dimers) in the Cu-ZSM-5 sample was explained with a two-step mechanism [19, 20], as shown in Equation (3) and (4)



whereas CuO particles are reduced with a one-step reduction [1, 21], as shown in Equation (5)



As illustrated in Fig. 4, all the catalysts show three H₂ consumption peaks at around 220, 330 and 580 °C, respectively, assigned to the reduction of one-step reduction of bulk CuO to Cu⁰ [19, 22], the reduction of the isolated Cu²⁺ ions to Cu⁺, and the

reduction of Cu^+ to Cu^0 [17, 20], respectively. Fig. 5 gives the ratio of the reducible Cu species calculated according to the deconvoluted peak areas of the H_2 -TPR plots. Surprisingly, the amount of the reduced Cu^+ are much more than the Cu^{2+} monomers reduced during the H_2 -TPR. The $(\text{Cu}^{2+}-\text{O}^{2-}-\text{Cu}^{2+})^{2+}$ is thermally unstable and is easily reduced to Cu^+ with deoxygenation at high temperatures in the pre-treatment in He before the H_2 -TPR [23]. In fact, the difference of the amount between the reduction of Cu^+ and Cu^{2+} during H_2 -TPR can be used to quantify the amount of $(\text{Cu}^{2+}-\text{O}^{2-}-\text{Cu}^{2+})^{2+}$ sites. Obviously, the Ni doped Ni-Cu-ZSM-5 and La-Ni-Cu-ZSM-5 contains more $(\text{Cu}^{2+}-\text{O}^{2-}-\text{Cu}^{2+})^{2+}$ sites than both Cu-ZSM-5 and La-Cu-ZSM-5, although the La-Cu-ZSM-5 contains more Cu^{2+} ions in total (including the monomer and the dimer) than Ni-Cu-ZSM-5, according to the Cu^+ amounts measured in Fig. 5.

3.4. NO-TPD

NO-TPD plots in Fig. 6 show four peaks with all the catalysts. The first peak at around 150 °C is assigned to the desorption of NO from the Cu^{2+} ions [20, 22]. The second peak at around 280 °C is attributed to the desorption of N_2O corresponding to the reaction between NO and $(\text{Cu}^+-\square-\text{Cu}^+)^{2+}$ [20], formed from $(\text{Cu}^{2+}-\text{O}^{2-}-\text{Cu}^{2+})^{2+}$ with the oxygen desorbed during the pretreatment in He at 500 °C. The desorption of N_2O also caused the recovery of the $(\text{Cu}^{2+}-\text{O}^{2-}-\text{Cu}^{2+})^{2+}$ dimer. The peak at around 350 °C is referred to the desorption of NO_2 corresponding to the reaction between NO and $(\text{Cu}^{2+}-\text{O}^{2-}-\text{Cu}^{2+})^{2+}$ [20]. The peak at around 390 °C is related to the decomposition of nitrate (NO_3^-) or nitrite (NO_2^-) caused by NO adsorption on $(\text{Cu}^{2+}-\text{O}^{2-}-\text{Cu}^{2+})^{2+}$ [24, 25].

It is clear that all the NO_x desorption peaks above 200 °C are related to the adsorption of NO on (Cu²⁺-O²⁻-Cu²⁺)²⁺, and the amounts of NO were calculated with integrating the convoluted peak areas and are shown in Fig. 7. La-Ni-Cu-ZSM-5 exhibits the largest NO_x desorption amount, as compared to the other catalyst samples.

3. 5. XPS

XPS technique was used to characterize the La and Ni state on the surface. Fig. 8 displays the core spectra of La 3d and exhibits asymmetric peaks at 835.8 and 852.8 eV for the 3d_{5/2} and 3d_{3/2} levels, respectively. The spin-orbit splitting is 17.1 eV, which are the characteristic of La³⁺. Moreover, both La 3d_{5/2} and 3d_{3/2} peaks exhibit “shake-up satellites” locating at a binding energy of 838.8 and 855.8 eV for the 3d_{5/2} and 3d_{3/2} levels, respectively, in the La doped samples. This multiple splitting peak was ascribed to the transfer of an electron from bonded oxygen to the empty La 4f state of La³⁺, indicating La³⁺ stays as La₂O₃ species on the external surface of the catalysts [26-30]. Fig. 9 indicates the absence of Ni species on the external surface of Ni-Cu-ZSM-5 and La-Ni-Cu-ZSM-5 catalysts [28].

3.6. NO Decomposition activity

The NO decomposition activity in the space velocity of 1200 h⁻¹ was adopted to study the effect of La and Ni on Cu-ZSM-5 in NO direct decomposition (Fig. S1), which is plotted in Fig. 10. H-ZSM-5 showed less than 8% NO conversion in the temperature range of 350 to 550 °C, which is consistent with the pervious works [31]. It is known that decomposition of NO to O₂ and N₂ is thermodynamically favorable, thus NO can

be slowly decomposed even in the absence of catalyst [32]. The low NO decomposition of the sample ZSM-5 is ascribed to the NO thermal decomposition. For the ZSM-5 doped with La and Ni, similar NO decomposition activity with that in the H-ZSM-5 sample was observed in 350-550 °C. This confirms the La and Ni is inactive for the NO decomposition.

For the samples with Cu loading, the NO conversion was 25% at 350 °C with Cu-ZSM-5, and then increased to 57% at 500 °C. The NO conversion decreased slightly to 55% with further increase of the temperature to 550 °C. The Ni-Cu-ZSM-5 sample shows enhanced NO decomposition performance as compared to that of the Cu-ZSM-5 sample in the temperature range of 350 to 550 °C. Meanwhile, the single doping of La (La-Cu-ZSM-5) caused slightly decrease of the NO conversion. Finally, La-Ni-Cu-ZSM-5 shows the best activity in 350-550 °C as compared to the Cu-ZSM-5 sample as well as to the single doped catalyst samples, showing 10% higher NO conversion than that in the Cu-ZSM-5 at 500 °C.

As shown in the Fig. 11, the TOF value decreased in an order of La-Ni-Cu-ZSM-5 > Ni-Cu-ZSM-5 > Cu-ZSM-5 > La-Cu-ZSM-5, identical with the sequence of NO decomposition activity curves. This indicates the co-doping of La and Ni or single doping with Ni is beneficial to the formation of active sites in Cu-ZSM-5.

4. Discussion

The N₂ physisorption results in Table 2 show identical surface areas and pore volumes with the doping of Ni and La and the co-doping of the two elements, indicating that the doping has no influence on the accessibility to the active sites in the pore structure. Meanwhile, Table 1 shows no significant change of the Cu content with the doping practice.

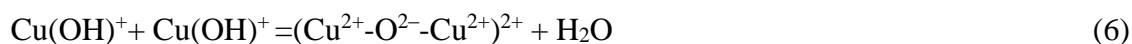
The XPS results in Fig. 8 shows that the La in the sample mainly exists as the La₂O₃ on the external surface. This result clearly demonstrates the failure of cation exchange of La ion into ZSM-5 with the ion exchange method. It is reported that the hydrolysis of La ion in aqueous solution is inevitable, and the La ion is hydrolyzed and stays as the [La(H₂O)₆]³⁺ during the ion-exchange procedure [33]. Moreover, the diameter of [La(H₂O)₆]³⁺ was estimated to be roughly 6.6 Å which is much larger than the pore size of NH₄-ZSM-5 (5.0 Å) as shown in Fig. 1 [34]. Hence, the ion exchange of La ion into the cage of ZSM-5 was hardly taken place, resulting in a large amount of La exists on the out surface of the samples. Similar phenomenon was also observed in the Cu-ZSM-5 samples doped with other lanthanide series elements such as Ce which possesses a similar size of the hydrated ions with La, where Ce predominately stays as the CeO₂ on the out surface of the zeolite crystallites [13].

The O₂-TPD curves in Fig. 3 show that two types of Cu²⁺ ions, the Cu²⁺ monomers and the (Cu²⁺-O²⁻-Cu²⁺)²⁺ dimers co-exist in all the catalyst samples. The La-Ni-Cu-ZSM-5 and La-Cu-ZSM-5 samples contain more Cu²⁺ ions than that in the Cu-ZSM-5

and Ni-Cu-ZSM-5 samples, according to the H₂-TPR result in Fig. 7. However, the total content of Cu is almost constant (Table 1) in all samples. This indicates the addition of La effectively improved the dispersion of the Cu species, which may be attributed to the preventing effect on the aggregation of the hydrated Cu²⁺ ions, thus reducing the bulk CuO content, which is consistent with the previously reported results [35, 36].

According to the XPS results in Fig. 9, no Ni was observed on the out surface of the Ni doped samples, whereas a low content of Ni was measured with ICP in the samples as the data given in Table 1. This suggests that Ni mainly exists in the inside of ZSM-5 crystallites. In comparison to the La ions, hydrated Ni ion processes a much smaller diameter (4.0 Å) [37], therefore, Ni ions can compete with the Cu²⁺ ions migrating into inside of the ZSM-5 crystallites to coordinate with the Al sites in the framework [38]. This may contribute to the reduced amount of the Cu²⁺ ions in the Ni-Cu-ZSM-5 sample, as compared to that in the Cu-ZSM-5 sample (Fig. 5).

Higher amounts of (Cu²⁺-O²⁻-Cu²⁺)²⁺ exist in La-Ni-Cu-ZSM-5 and Ni-Cu-ZSM-5 samples than those in the Cu-ZSM-5 and La-Cu-ZSM-5 samples, according to the H₂-TPR results presented in Fig. 5. The (Cu²⁺-O²⁻-Cu²⁺)²⁺ may be formed due to the dehydration of the adjacent Cu²⁺ ions (stay as Cu(OH)⁺) follow the reaction: [19, 39-41].



Consequently, the doping of Ni may occupy the sites for copper ion-exchange, causing the increase of (Cu²⁺-O²⁻-Cu²⁺)²⁺ and the decrease of the Cu²⁺ monomer.

In short, La promotes the dispersion of the cupric species, whereas Ni promotes the formation of the $(\text{Cu}^{2+}\text{-O}^{2-}\text{-Cu}^{2+})^{2+}$ dimers. The co-promotion of La and Ni in La-Ni-Cu-ZSM-5 results in the highest content of the $(\text{Cu}^{2+}\text{-O}^{2-}\text{-Cu}^{2+})^{2+}$ dimer, as shown in Fig. 5. This proposition is schematically presented in Fig. 12.

As shown in Fig. 10 and Fig. 11, the activity of NO decomposition and the TOF value decreased in an order of La-Ni-Cu-ZSM-5 > Ni-Cu-ZSM-5 > Cu-ZSM-5 > La-Cu-ZSM-5, identical with the sequence of the $(\text{Cu}^{2+}\text{-O}^{2-}\text{-Cu}^{2+})^{2+}$ dimer content estimated based on H_2 -TPR in Fig. 5. This indicates the Cu-dimer is the major active sites for NO direct decomposition, whereas it seems the Cu^{2+} monomer is not relevant with the NO reduction. This remark is consistent with the previous works [20, 40]. It is well known that the NO decomposition activity is highly relevant to the activation of NO on the Cu sites [15]. NO-TPD in Fig. 6 shows all the NO_x released above 200 °C is produced with desorption or surface reaction of NO on the Cu-dimer sites. On the other hand, almost no NO_x desorbed from the Cu^{2+} monomer. This is likely related to the unstable oxygen in the Cu-dimer, as shown in O_2 -TPD in Fig. 3. In contrast, the neighboring oxygen of the Cu^{2+} monomers are very stable, inactive with the activation of NO [42]. Apparently, further effort is needed to optimize the La/Ni ratio for the optimum $(\text{Cu}^{2+}\text{-O}^{2-}\text{-Cu}^{2+})^{2+}$ dimer content, for the best NO decomposition activity.

5. Conclusion

This contribution shows different effect of La and Ni on Cu-ZSM-5 as structural and chemical promoters. La promotes the dispersion of the cupric species, resulting in high content of Cu^{2+} ions, whereas Ni promotes the formation of the $(\text{Cu}^{2+}-\text{O}^{2-}-\text{Cu}^{2+})^{2+}$ dimers as the major active sites for NO direct decomposition. The result shows that the co-doped La-Ni-Cu-ZSM-5 catalyst takes the synergistic effects of the two promoters, resulting in the highest dimer content as well as the highest activity of NO direct decomposition.

Acknowledgments

This work was supported in part by the Program of Introducing Talents to the University Disciplines under file number B06006, and the Program for Changjiang Scholars and Innovative Research Teams in Universities under file number IRT 0641.

Reference

- [1] H. Zhao, H. Li, X. Li, M. Liu, Y. Li, *Catal. Today* 297 (2017) 84-91.
- [2] J. Wang, H. Zhao, G. Haller, Y. Li, *Appl. Catal. B: Environ.* 202 (2017) 346-354.
- [3] D. Mráček, P. Kočí, J. S. Choi, W. P. Partridge, *Appl. Catal. B: Environ.* 182 (2016) 109-114.
- [4] M. Iwamoto, H. Yahiro, K. Tanda, N. Mizuno, Y. Mine, S. Kagawa, *Cheminform* 22 (1991) 3727-3730.
- [5] T. Masui, S. Uejima, S. Tsujimoto, R. Nagai, N. Imanaka, *Catal. Today* 242 (2015) 338-342.
- [6] L. Chen, X. Niu, Z. Li, Y. Dong, D. Wang, F. Yuan, Y. Zhu, *J. Mol. Catal. A: Chem.* 423 (2016) 277-284.
- [7] K. Zha, S. Cai, H. Hu, H. Li, T. Yan, L. Shi, D. Zhang, *J. Phys. Chem. C* (2017) 25243-25254.
- [8] L. Yan, Y. Liu, K. Zha, H. Li, L. Shi, D. Zhang, *ACS Appl. Mater. Inter.* 9 (2017) 2581-2593.
- [9] M. Iwamoto, H. Furukawa, Y. Mine, F. Uemura, S. Mikuriya, S. Kagawa, *J. Chem. Soc. Chem. Commun.* 16 (1986) 1272-1273.
- [10] R. Burch, T. C. Watling, *Catal. Lett.* 37 (1996) 51-55.
- [11] M. Iwamoto, H. Yahiro, K. Tanda, N. Mizuno, Y. Mine, S. Kagawa, *Cheminform* 95 (1991) 3727-3730.
- [12] R. Zhang, N. Liu, Z. Lei, B. Chen, *Chem. Rev.* 116 (2016) 3658.

- [13] Y. Zhang, M. Flytzani-Stephanopoulos, *J. Catal.* 164 (1996) 131-145.
- [14] V. I. Pârvulescu, P. Oelker, P. Grange, B. Delmon, *Appl. Catal. B: Environ.* 16 (1998) 1-17.
- [15] V. I. Pârvulescu, P. Grange, B. Delmon, *Appl. Catal. B: Environ.* 33 (2001) 223-237.
- [16] B. Ganemi, E. Björnbo, B. Demirel, J. Paul, *Microporous Mesoporous Mater.* 38 (2000) 287-300.
- [17] Y. Teraoka, C. Tai, H. Ogawa, H. Furukawa, S. Kagawa, *Appl. Catal. A: Gen.* 200 (2000) 167-176.
- [18] P. D. Costa, B. Modén, G. D. Meitzner, D. K. Lee, E. Iglesia, *Phys. Chem. Chem. Phys.* 4 (2002) 4590-4601.
- [19] J. Sárkány, J. L. D'Itri, W. M. H. Sachtler, *Catal. Lett.* 16 (1992) 241-249.
- [20] D. K. Lee, *Korean J. Chem. Eng.* 21 (2004) 611-620.
- [21] J. Xue, X. Wang, G. Qi, J. Wang, M. Shen, W. Li, *J. Catal.* 297 (2013) 56-64.
- [22] C. Torre-Abreu, M. F. Ribeiro, C. Henriques, G. Delahay, *Appl. Catal. B: Environ.* 12 (1997) 249-262.
- [23] H. Yahiro, T. Nagano, H. Yamaura, *Catal. Today* 126 (2007) 284-289.
- [24] W. X. Zhang, H. Yahiro, N. Mizuno, M. Iwamoto, J. Izumi, *J. Mater. Sci. Lett.* 12 (1993) 1197-1198.
- [25] B. Modén, P. D. Costa, B. Fonfé, D. K. Lee, E. Iglesia, *J. Catal.* 209 (2002) 75-86.
- [26] E. Beyreuther, S. Grafström, L. M. Eng, C. Thiele, K. Dörr, *Phys. Rev. B* 81 (2006)

155425.

- [27] S. Suga, S. Imada, T. Muro, T. Fukawa, T. Shishidou, Y. Tokura, Y. Moritomo, T. Miyahara, J. Electron. Spectrosc. Relat. Phenom. 78 (1996) 283-286.
- [28] M. He, X. Wang, L. Zhang, Q. Wu, X. Song, A. I. Chernov, P. V. Fedotov, E. D. Obraztsova, J. Sainio, H. Jiang, H. Cui, F. Ding, E. Kauppinen, Carbon 128 (2018) 249-256.
- [29] C. N. Borca, S. Canulescu, F. Loviat, T. Lippert, D. Grolimund, M. Döbeli, J. Wambach, A. Wokaun, Appl. Surf. Sci. 254 (2007) 1352-1355.
- [30] M. F. Sunding, K. Hadidi, S. Diplas, O. M. Løvvik, T. E. Norby, A. E. Gunnæs, J. Electron. Spectrosc. 184 (2011) 399-409.
- [31] Y. F. Chang, J. G. Mccarty, J. Catal. 178 (1998) 408-413.
- [32] C. T. Goralski Jr, W. F. Schneider, Appl. Catal. B: Environ. 37 (2002) 263-277.
- [33] P. Tynjälä, T. T. Pakkanen, J. Mol. Catal. A: Chem. 110 (1996) 153-161.
- [34] R. Zhang, N. Liu, Z. Lei, B. Chen, Chem. Rev. 116 (2016) 3658-3721.
- [35] L. Huang, X. Wang, S. Yao, B. Jiang, X. Chen, X. Wang, Catal. Commun. 81 (2016) 54-57.
- [36] Y. Cao, X. Feng, H. Xu, L. Lan, M. Gong, Y. Chen, Catal. Commun. 76 (2016) 33-36.
- [37] A. G. Volkov, S. Paula, D. W. Deamer, Bioelectrochemistry 42 (1997) 153-160.
- [38] G. Moretti, Catal. Lett. 28 (1994) 143-152.
- [39] W. P. J. H. Jacobs, J. H. M. C. V. Wolput, R. A. V. Santen, Zeolites 13 (1993) 170-182.

[40] P. D. Costa, B. R. Modn, G. D. Meitzner, D. K. Lee, E. Iglesia, *Phys. Chem. Chem. Phys.* 4 (2002) 4590-4601.

[41] B. Wichterlova, J. Dedecek, A. Vondrova, *J. Phys. Chem.* 99 (1995) 1065-1067.

[42] A. A. Verma, S. A. Bates, T. Anggara, C. Paolucci, A. A. Parekh, K. Kamasamudram, A. Yezerets, J. T. Miller, W. N. Delgass, W. F. Schneider, F. H. Ribeiro, *J. Catal.* 312 (2014) 179-190.

Table 1. La, Ni and Cu contents of the M-Cu-ZSM-5 (M=La, Ni, La-Ni) samples determined with ICP.

Sample	Cu content ^a wt. %	Al content ^a wt. %	Cu exchange level ^b %	La content ^a wt. %	Ni content ^a wt. %
Cu-ZSM-5	3.23	2.42	113	0	0
Ni-Cu-ZSM-5	3.18	2.46	109	0	0.035
La-Cu-ZSM-5	3.11	2.49	105	0.033	0
La-Ni-Cu-ZSM-5	3.06	2.51	103	0.026	0.025

^a Determined with the ICP.

^b Two times Molar ratio of Cu to total Al.

Table 2. The BET result for the M-Cu-ZSM-5 (M=La, Ni and La-Ni) samples.

Sample	Surface area ^a m ² /g	Pore volume ^b cm ³ /g
Cu-ZSM-5	272	0.17
Ni-Cu-ZSM-5	259	0.16
La-Cu-ZSM-5	267	0.17
La-Ni-Cu-ZSM-5	247	0.15

^a Determined with the BET equation.

^b Calculated with the t-plot method.

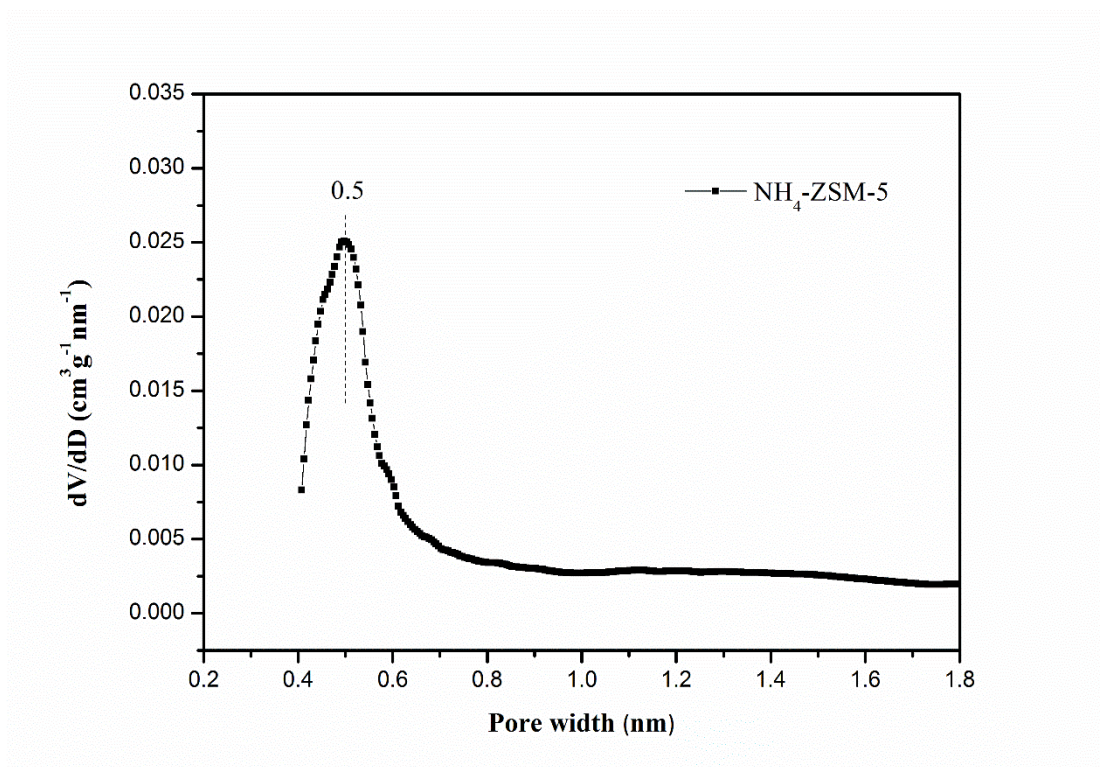


Fig. 1. Micropore size distribution of NH₄-ZSM-5 sample determined with the Horvath-Kawazoe methods

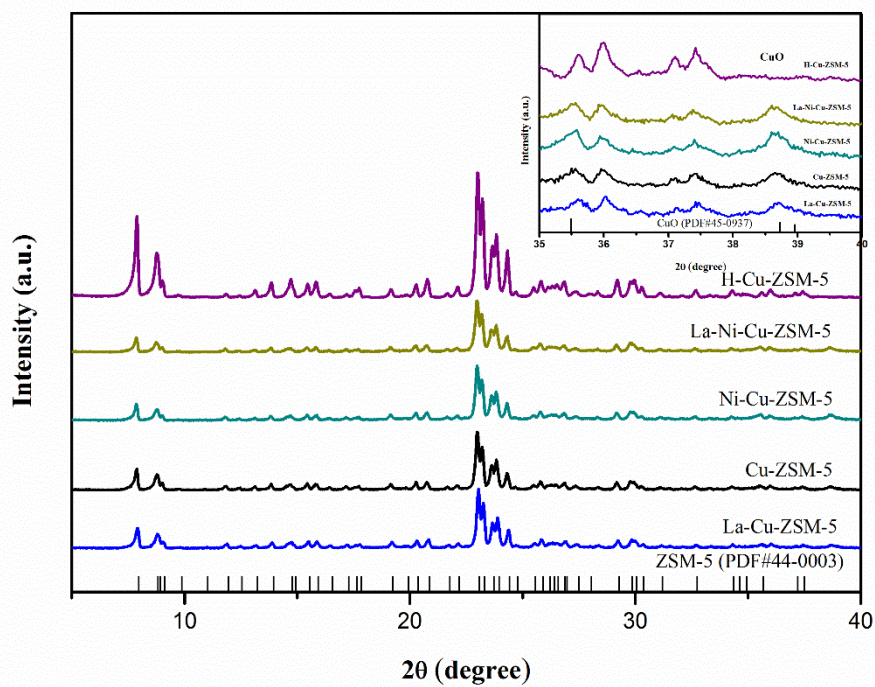


Fig. 2. XRD patterns for the M-Cu-ZSM-5 (M=La, Ni, La-Ni) samples. The insert is the XRD patterns of CuO.

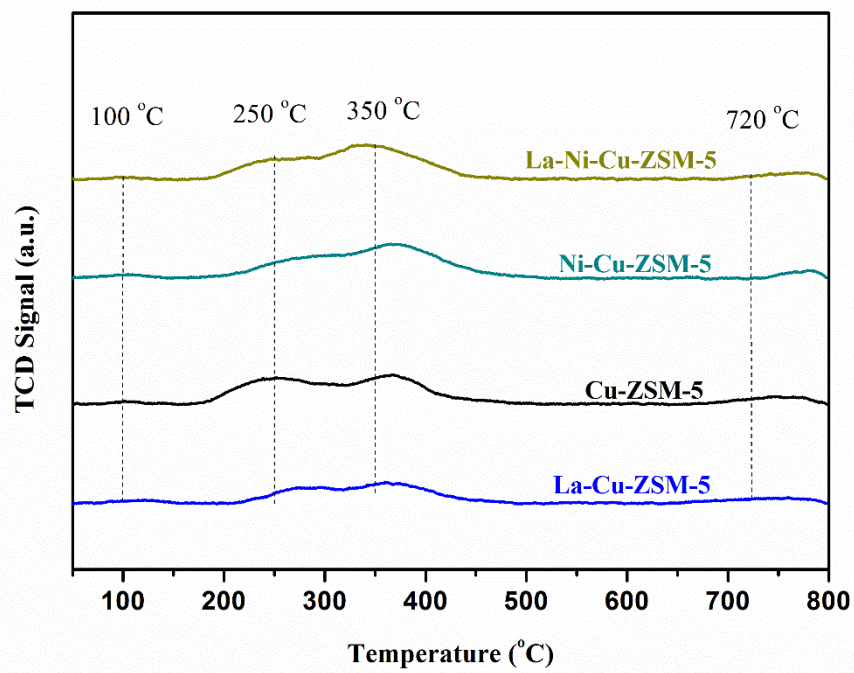


Fig. 3. O₂ temperature-programmed desorption (O₂-TPD) profiles of the M-Cu-ZSM-5 (M=La, Ni, La-Ni) samples.

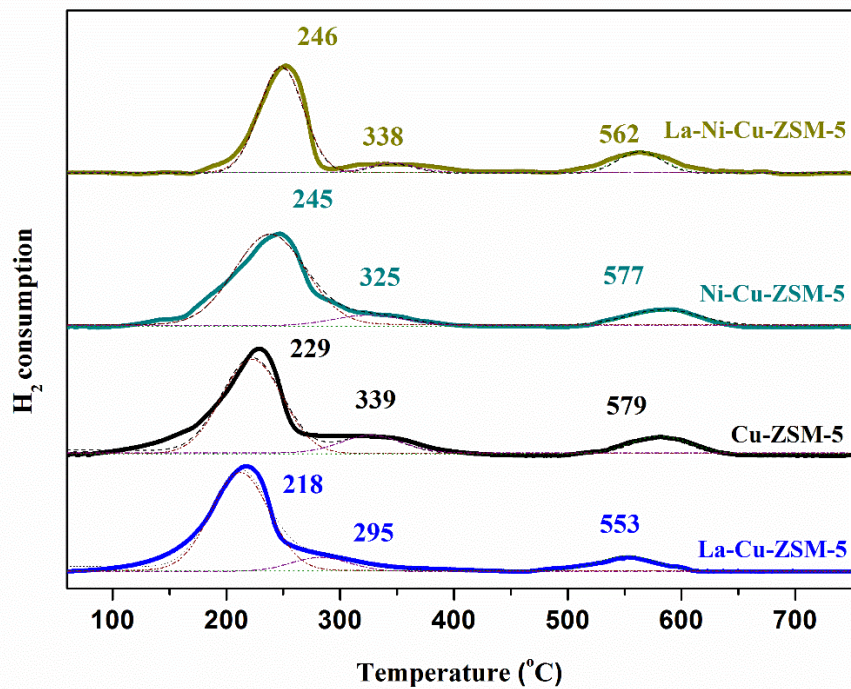


Fig. 4. H₂ temperature-programmed reduction (H₂-TPR) curves for the M-Cu-ZSM-5 (M=La, Ni, La-Ni) samples. The wine dotted line represents the H₂ consumption of CuO. The purple dotted line represents the H₂ consumption of Cu²⁺. The olive dotted line represents the H₂ consumption of Cu⁺.

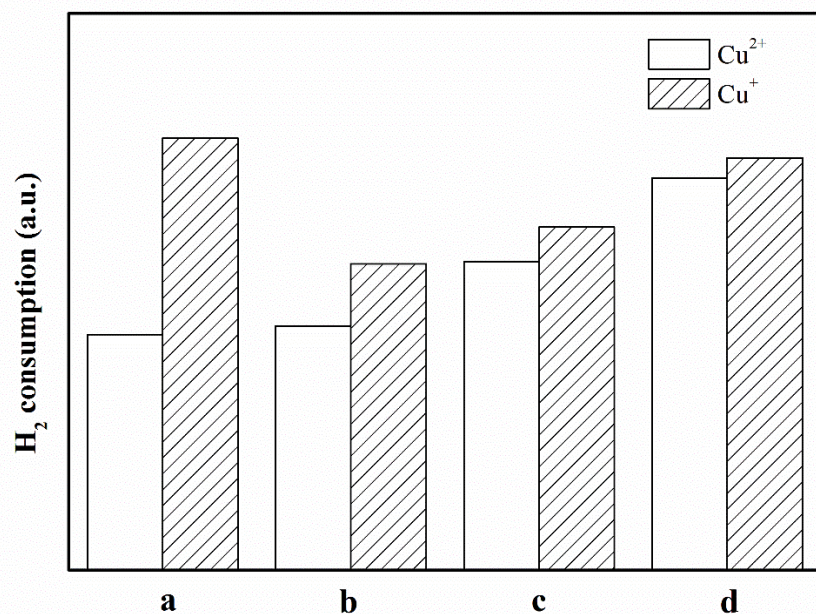


Fig. 5. The amount of H₂ consumption related to isolated Cu²⁺ and Cu⁺ of the H₂-TPR of (a) La-Ni-Cu-ZSM-5, (b) Ni-Cu-ZSM-5, (c) Cu-ZSM-5, (d) La-Cu-ZSM-5. The amount of Cu⁺ indicates the total amount of isolated Cu²⁺ ions (including monomer and dimer), and the amount of Cu²⁺ indicates amount of Cu²⁺ monomer exclusively.

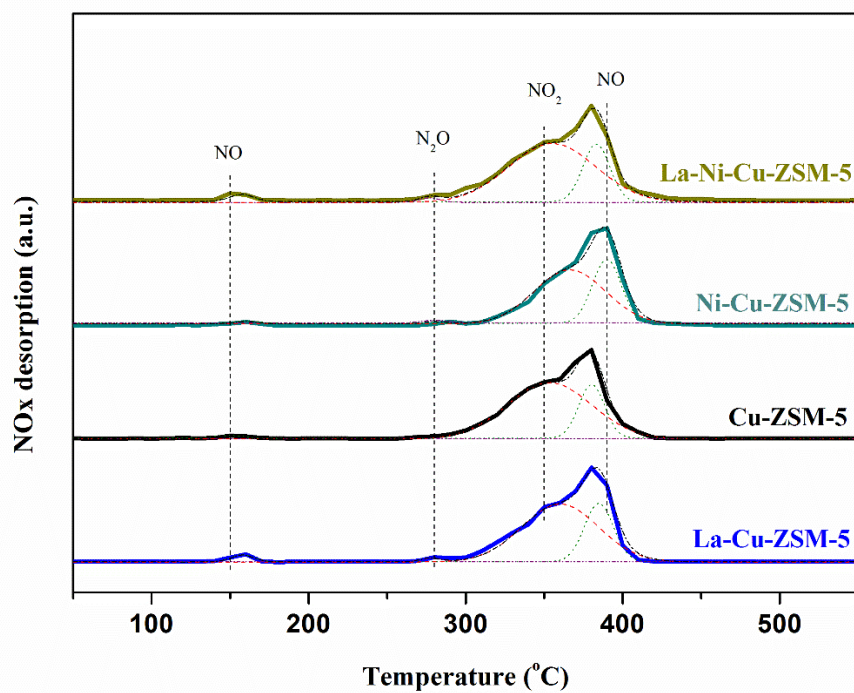


Fig. 6. NO_x temperature-programmed desorption (NO_x-TPD) curves for the M-Cu-ZSM-5 (M=La, Ni, La-Ni) samples. The red dotted line represents the NO₂ desorption. The purple dotted line represents the N₂O desorption. The olive dotted line represents the NO desorption.

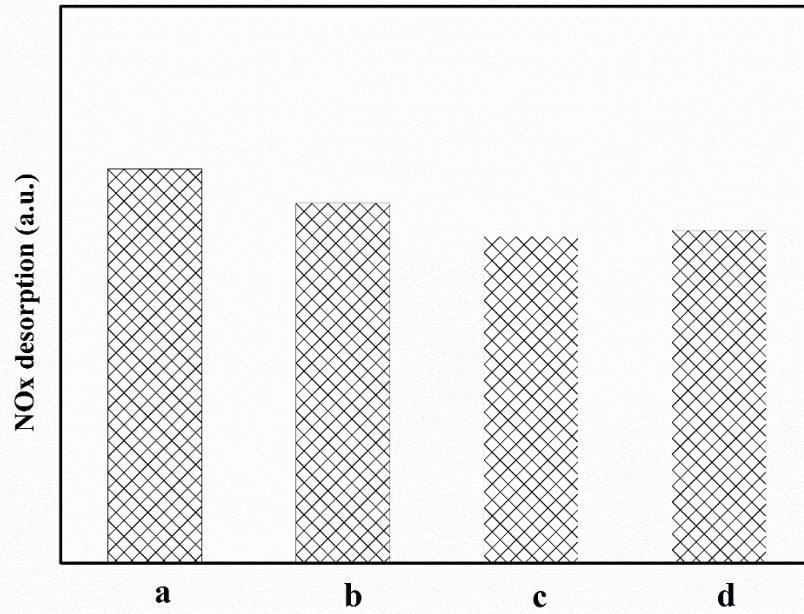


Fig. 7. The amount of NO_x desorption of the NO_x-TPD of (a) La-Ni-Cu-ZSM-5, (b) Ni-Cu-ZSM-5, (c) Cu-ZSM-5, (d) La-Cu-ZSM-5.

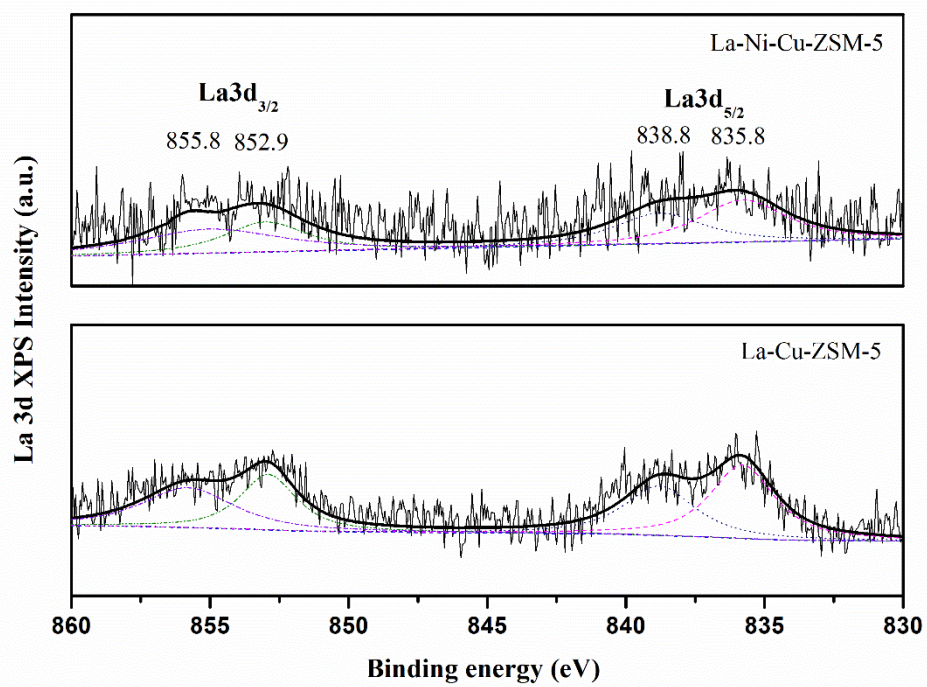


Fig. 8. La 3d XPS spectra of La-Ni-Cu-ZSM-5 and La-Cu-ZSM-5 samples.

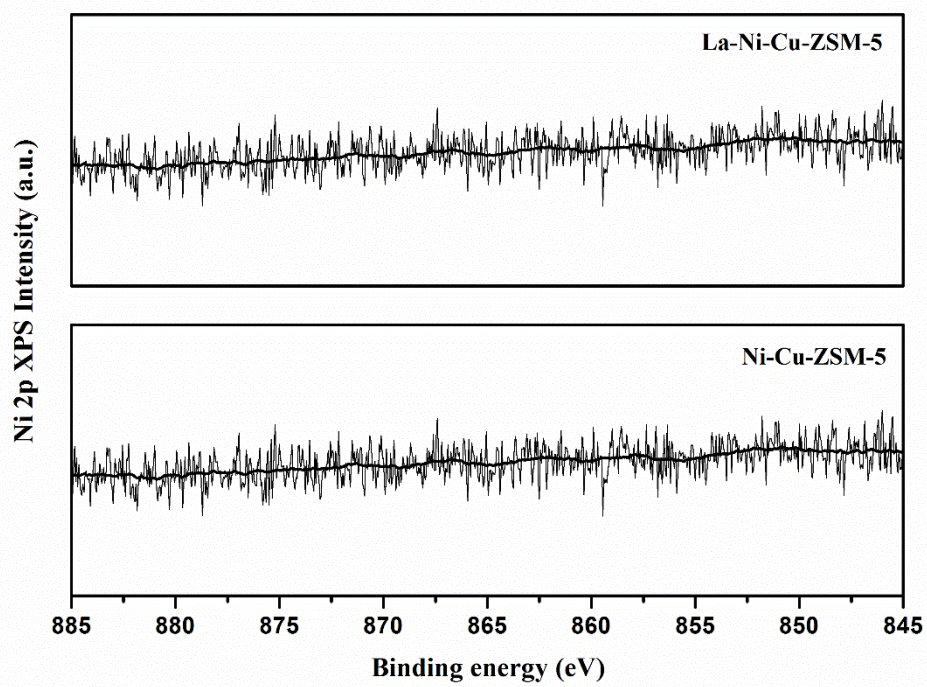


Fig. 9. Ni 2p XPS spectra of the La-Ni-Cu-ZSM-5 and Ni-Cu-ZSM-5 samples.

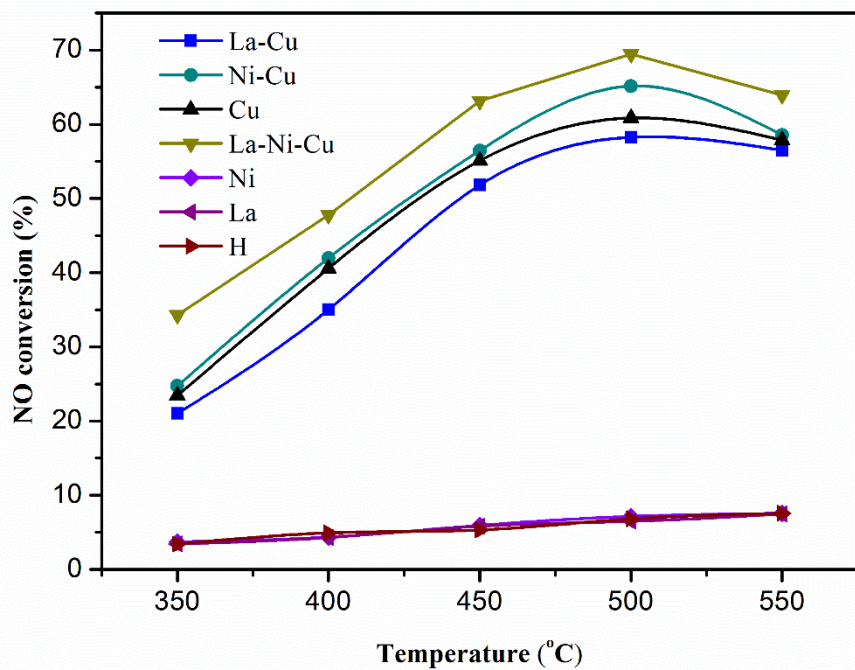


Fig. 10. NO conversion ($\frac{2 [N_2]_{out}}{[NO]_{in}} \times 100\%$) as a function of the temperature (350–550 °C) of the M-Cu-ZSM-5 (M=H, La, Ni, La-Ni) samples.

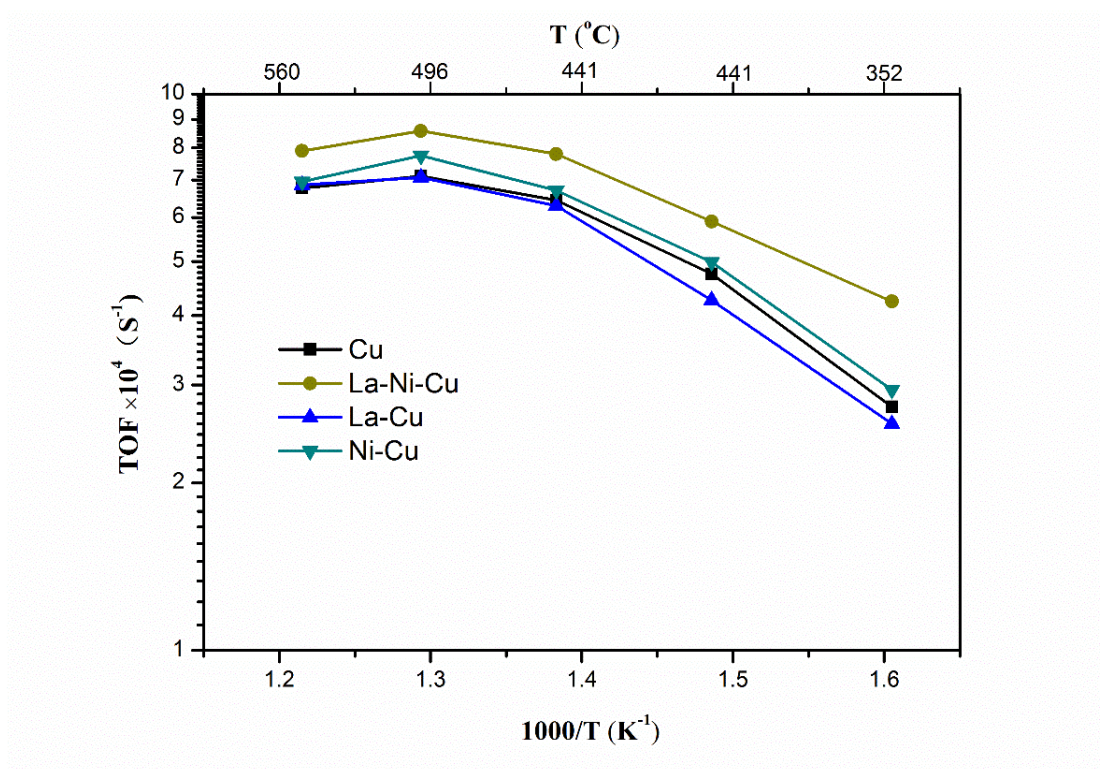


Fig.11. Arrhenius plot illustrating the activity difference between La-Ni-Cu-ZSM-5, Ni-Cu-ZSM-5, La-Cu-ZSM-5 and Cu-ZSM-5. The inlet concentration of NO was 2 vol.% in He.

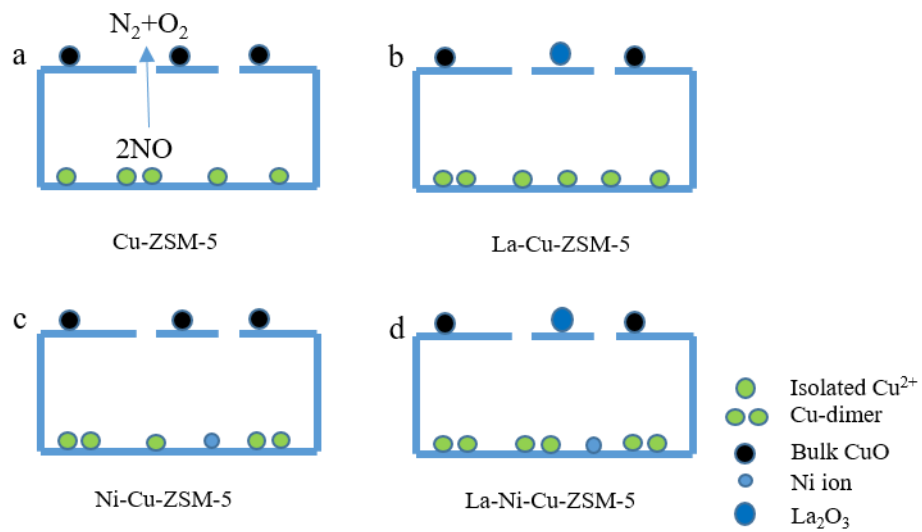


Fig. 12. The effect of the promoters (La, Ni and La-Ni) on the nature of the Cu in Cu-ZSM-5.

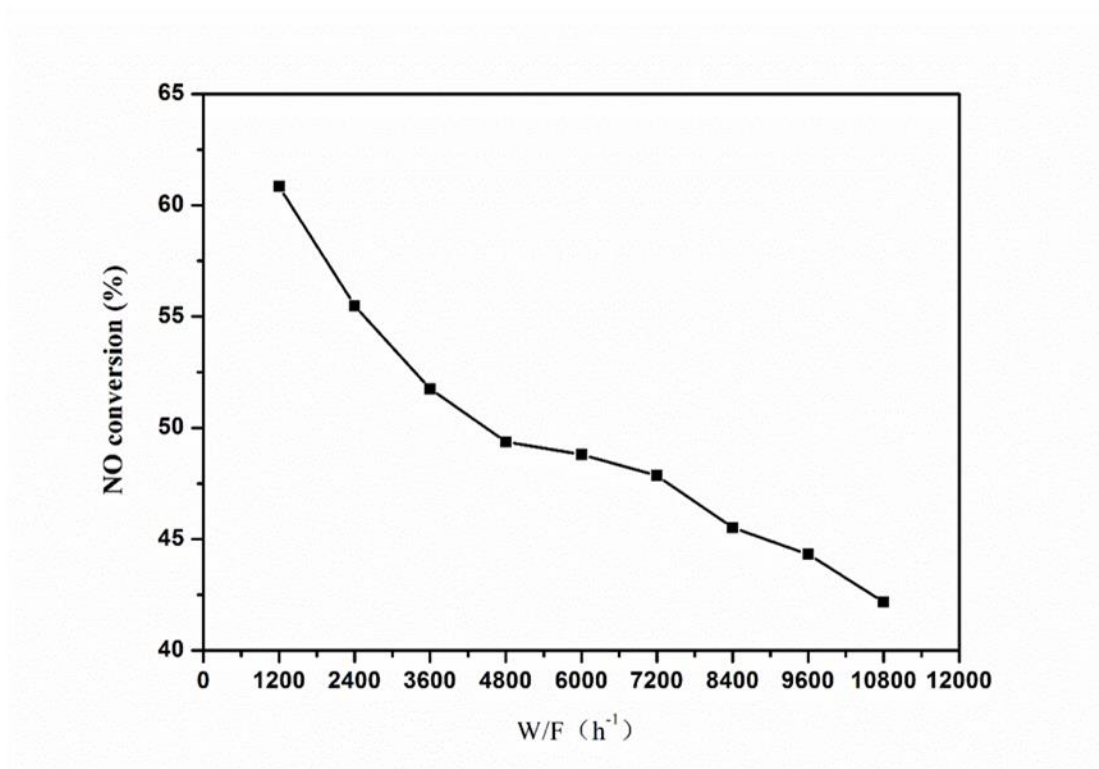


Fig. S1 Effect of space velocity on catalytic activity of Cu-ZSM-5.

The Fig. S1 shows the NO_x conversion at 500 °C versus space velocity for NO decomposition over the Cu-ZSM-5. The NO conversion decreased with the increase of the space velocity. The appropriate NO conversion is necessary study the promotion effect of La and Ni on Cu-ZSM-5 in NO direct decomposition, which is consistent with the pervious works [1-3]. Hence, the GHSV of 1200 h⁻¹ was adopted in this work.

References

- [1] Y. Zhang, M. Flytzani-Stephanopoulos, *J. Catal.* 164 (1996) 131-145.
- [2] V. I. Pârvulescu, P. Oelker, P. Grange, B. Delmon, *Appl. Catal. B: Environ.* 16 (1998) 1-17.
- [3] M. H. Groothaert, J. A. van Bokhoven, A. A. Battiston, B. M. Weckhuysen, R. A. Schoonheydt, *J. Am. Chem. Soc.* 125 (2003) 7629-7640.